

# **Electronic excitations in nonpolar solvents: can the Polarizable Continuum Model accurately reproduce solvent effects?**

Lorenzo Cupellini,\* Claudio Amovilli,\* and Benedetta Mennucci\*

*Dipartimento di Chimica e Chimica Industriale, University of Pisa, Via Risorgimento 35, 56126  
Pisa, Italy*

E-mail: [lorenzo.cupellini@for.unipi.it](mailto:lorenzo.cupellini@for.unipi.it); [claudio.amovilli@unipi.it](mailto:claudio.amovilli@unipi.it); [benedetta.mennucci@unipi.it](mailto:benedetta.mennucci@unipi.it)

---

\*To whom correspondence should be addressed

## Abstract

In nonpolar solvents, both electrostatic and nonelectrostatic interactions play a role in tuning the electronic excitations of molecular solutes. This specificity makes the application of continuum solvation models a challenge. Here, we propose a strategy for the calculation of solvatochromic shifts on absorption spectra, using a coupling of the Polarizable Continuum Model with a time-dependent DFT framework which explicitly accounts for dispersion and repulsion, as well as for electrostatic effects. Our analysis makes a step further in the interpretation of the effects of nonpolar solvents and suggests new directions in their modeling using continuum formulations.

**Keywords:** solvatochromism, dispersion effects, electrostatic effects, polarizable continuum model

## 1 Introduction

Environmental effects play a crucial role in tuning the optical properties of molecules and the corresponding electronic spectroscopies. In quantum chemistry, these effects are commonly dealt with by introducing an interaction term in the molecular Hamiltonian, as in the so-called *effective Hamiltonian* methods. These methods include both the quantum mechanics/molecular mechanics (QM/MM) models, which adopt a classical but atomistic description of the environment<sup>1-6</sup>, and the QM/continuum models, which describe implicitly the environment as a structureless dielectric medium.<sup>7-11</sup> Both QM/MM and QM/continuum models have in common the classical electrostatic nature of the QM/classical interaction potential. On the contrary, nonelectrostatic interactions (namely dispersion and repulsion) are usually associated to classical potentials, disregarding their quantum-mechanical origin; dispersion is indeed a nonlocal electron correlation effect, while repulsion arises from the Pauli exclusion principle. Attempts to describe dispersion and repulsion effects through quantum-mechanical approaches have already been proposed within QM/continuum models. The self-consistent model of Amovilli and Mennucci<sup>12</sup> developed

reformulating the theory of weakly interacting systems within the Polarizable Continuum Model (PCM)<sup>11</sup> is an example of such attempts, together with the model recently developed by Pomogaeva and Chipman from a density functional formulation of dispersion energy.<sup>13,14</sup>

In the large majority of cases, however, both QM/MM and QM/continuum models have been employed in the treatment of solvent effects on electronic spectroscopies such as absorption, fluorescence, and circular dichroism by limiting the solute-solvent interactions to the electrostatic one.<sup>5,15,16</sup> On the contrary, nonelectrostatic interactions, and particularly dispersion, are expected to significantly affect the electronic spectra in solution, especially when the solvent is nonpolar. In 1950, Bayliss proposed the first continuum model to explain the dispersion shift in nonpolar solvents, which was related to the oscillator strength of the transition and to the square of the refractive index.<sup>17</sup> Another approach was proposed by Rösch and Zerner within a QM description by calculating dispersion effects on the excitation energies as difference in the dispersion stabilization energy from ground to excited state obtained at a semiempirical configuration interaction (CIS) treatment of both solute and solvent molecules.<sup>18</sup> In more recent years, the interest in the modeling of dispersion effects on solvatochromic shifts has grown further, and several steps ahead have been made. A semiclassical expression has been derived by Renger *et al.*<sup>19</sup>, under a dipole approximation. The model by Amovilli and Mennucci<sup>12</sup> has been extended to electronic excitations by Weijo *et al.*<sup>20</sup>. More recently, Marenich *et al.*<sup>21</sup> proposed a state-specific polarizability model (SMSSP) for dispersion and applied that to the calculation of solvatochromic shifts of aromatic hydrocarbons in nonpolar solvents. **The SMSSP model was successively coupled to a state-specific description of the electrostatic effects in order to calculate solvatochromic shifts of polar chromophores in water and methanol.**<sup>22</sup>

All these developments have lead us to reconsider the problem of the applicability of continuum models to describe solvent effects in the excitations of molecular solutes in nonpolar solvents. In particular, we focus here on the PCM formulation of continuum models and we investigate the contribution that each interaction (electrostatic, repulsive and dispersive) has on the excitation

energies of valence transitions of a selected set of polar and apolar solutes in a nonpolar solvent and the possible couplings among them. This analysis is performed applying the time-dependent formulation of Density Functional Theory (DFT) and the role played by the chosen functional is evaluated together with the impact that different formulations of the electrostatic contribution have on the accuracy of the correlation with experimental solvatochromic shifts.

The paper is organized as follows. In Sec. 2, we present the methodological aspects related to the calculation of solvent effects in electronic excitations with the PCM, in Sec. 3 we report the computational details and, in Sec. 4, we present a detailed analysis of the results. We conclude with a brief summary in Sec. 5.

## 2 Methods

In short, the PCM description of the electrostatic solute-solvent interaction including polarization effects is through the introduction of an apparent surface charge (ASC) density  $\sigma$  supported on the surface  $\Gamma$  of the cavity which contains the QM solute:

$$W_{ele} = \int_{\Gamma} ds \sigma[\epsilon, \rho](s) V[\rho](s) \quad (1)$$

where  $V[\rho]$  is the electrostatic potential generated by the QM solute (here represented in terms of its charge distribution  $\rho$ ) and  $\epsilon$  is the solvent dielectric constant.  $\sigma$  is obtained as the solution of a specific integral equation: various alternative expressions of this equation have been given during the years leading to different formulations of the PCM, known as D-PCM,<sup>23,24</sup> C-PCM<sup>25</sup> and IEF-PCM.<sup>26</sup> In all cases, the surface charge will depend on the shape of the cavity and on the electrostatic potential (or field) generated by the QM solute on the surface. Commonly, a numerical representation of  $\sigma$  is used introducing a mesh of the cavity surface and replacing the continuous ASC distribution with point like charges.

Moving to **Pauli** repulsion and dispersion interactions, the Amovilli and Mennucci’s approach<sup>12</sup> is here adopted. In short, the **Pauli** repulsion contribution is derived from the exchange and penetration terms of the decomposition of the intermolecular interaction energy. A simplified expression for a uniform solvent, which takes into account its continuum nature is then obtained:

$$W_{rep} = k_{rep} \frac{\rho_S n_S^v}{M_S} \int_{r \notin C} dr \rho(r) \quad (2)$$

where  $k_{rep}$  is a suitable scaling parameter,  $\rho_S$  the density of the solvent relative to water at 298 K,  $n_S^v$  the number of valence electrons in the solvent molecules, and  $M_S$  their molecular weight. Eq. (2) shows that the repulsion interaction is proportional to the so called “escaped charge”: the electronic density which extends beyond the boundaries of the molecular cavity.

The expression for the dispersion energy is instead achieved by similarity with electrostatics introducing another ASC density induced on the cavity surface by the transition charge density  $\rho_p$  and depending on a dielectric constant calculated at imaginary frequencies,  $\varepsilon(i\omega)$ . By assuming  $\sigma[\varepsilon(i\omega), \rho_p]$ <sup>27</sup> to be proportional to the corresponding electrostatic field generated by  $\rho_p$ , the interaction energy can be written as:<sup>12</sup>

$$W_{disp} = -k_{disp} \frac{\eta_S^2 - 1}{\eta_S^2} \sum_p \frac{\Omega^S}{\Omega^S + \omega_p} \int_{\Gamma} ds V_p(s) E_p(s) \quad (3)$$

where the index  $p$  runs over the excited states of the solute,  $\omega_p$  is the corresponding excitation energy and  $V_p$  and  $E_p$  are the electrostatic potential and the normal component of the electrostatic field generated on the surface by the transition density, respectively.  $\eta_S$  is the solvent refractive index measured in the visible spectrum far from electron transitions whereas  $\Omega^S = \eta_S I$ , with  $I$  being the first ionization potential of the solvent. In order to achieve a practical expression, a further simplification is introduced, by making use of an averaged excitation energy  $\omega_{ave}$ , thereby eliminating the dependence of the prefactor of the surface integral on the excited state in Eq. (3). We also note that the parameter  $k_{disp}$ <sup>12</sup> was originally determined using Hartree-Fock calculations and the aver-

aged excitation energy  $\omega_{\text{ave}}$  was obtained by considering a predefined set of occupied and virtual orbitals defined by a window of energies and averaging for such a set. This choice is, however, strictly connected to the QM method employed.<sup>28</sup> In order to avoid that, a new parameterization has been more recently proposed<sup>20</sup> and the parameter  $k_{\text{disp}}$  is chosen to be solvent-dependent.

Each of the three interactions corresponds to a term in the effective Hamiltonian such that, electrostatic, dispersion and repulsion effects will contribute to determine the solute wavefunction and the corresponding electron density. Moreover, the resulting effective Hamiltonian can also be generalized to calculate solvent effects on excitation energies using the common approaches developed for gas-phase molecules.

During the years, different strategies have been proposed to account for solvent effects on excitations using a PCM approach. The differences among the strategies arise not only from the type of interactions included (only electrostatic, electrostatic plus dispersion and repulsion) but also from the formulation used for the electrostatic contribution. These different formulations can be collected in two main families, the so-called linear response (LR)<sup>29,30</sup> and state-specific (SS)<sup>31–33</sup> approaches. By simplifying at most, we can say that in the LR formulation, the response of the solvent polarization to a given excitation  $p$  is computed from the transition density  $\rho_p$  (Eq. (4)), while in the SS approach the same polarization is determined by the difference between ground and excited state electron density  $\rho_{\Delta p}$  (Eq. (5)):

$$\omega_{LR} = \omega_0 + \int_{\Gamma} V[\rho_p](s) \sigma[\epsilon_{\infty}, \rho_p](s) ds \quad (4)$$

$$\omega_{SS} = \omega_0 + \frac{1}{2} \int_{\Gamma} V[\rho_{\Delta p}](s) \sigma[\epsilon_{\infty}, \rho_{\Delta p}](s) ds \quad (5)$$

where in both cases a nonequilibrium response of the solvent has been used by introducing an optical dielectric constant  $\epsilon_{\infty}$ : this is justified if we describe the excitation as a vertical process and we assume that only the fast (or electronic) part of the solvent polarization will respond. In the two equations,  $\omega_0$  is the same quantity and it represents a “frozen solvent” contribution.

In the above equations nonelectrostatic effects are not explicitly accounted for. **Since the repulsion operator (derived from the interaction energy Eq. (2)) is an one-electron operator, repulsion does not give any explicit term in Eqs. (4) and (5). However, the repulsion operator changes the ground-state orbitals, thus implicitly affecting  $\omega$  through  $\omega_0$  and  $\rho_{\Delta p}$  or  $\rho_p$ .** On the contrary, dispersion gives an explicit contribution (in addition to the implicit one): due to the nature of the expression here used (see Eq. (3)), this contribution is independent of the LR or SS scheme (see below).

If we now apply a TD-DFT framework, the LR transition energies and transition densities are obtained as eigenvalues and eigenvectors of the non-Hermitian eigensystem:

$$\begin{bmatrix} \mathbb{A} & \mathbb{B} \\ \mathbb{B}^* & \mathbb{A}^* \end{bmatrix} \begin{bmatrix} \mathbf{X} \\ \mathbf{Y} \end{bmatrix} = \omega_{LR} \begin{bmatrix} \mathbb{1} & 0 \\ 0 & -\mathbb{1} \end{bmatrix} \begin{bmatrix} \mathbf{X} \\ \mathbf{Y} \end{bmatrix} \quad (6)$$

$\mathbb{A}$  and  $\mathbb{B}$  being

$$\begin{aligned} \mathbb{A}_{ai,bj} &= \delta_{ab}\delta_{ij}(\epsilon_a - \epsilon_i) + \langle ia | jb \rangle + f_{ai,bj}^{xc} + V_{ai,bj}^{PCM} \\ \mathbb{B}_{ai,bj} &= \langle ia | bj \rangle + f_{ai,bj}^{xc} + V_{ai,bj}^{PCM} \end{aligned} \quad (7)$$

where indices  $i, j, \dots$  label occupied, and  $a, b, \dots$  virtual molecular orbitals and  $\epsilon_r$  are the corresponding orbital energies as obtained for the solvated ground state solute. In Eq. (7)  $f_{ai,bj}^{xc}$  represents a matrix element of the exchange-correlation kernel in the adiabatic approximation while  $V_{ai,bj}^{PCM}$  is the corresponding matrix element of the PCM reaction potential which can be obtained as second derivative with respect to the density of the electrostatic interaction energy reported in Eq. (1). In the same way we can also introduce dispersion effects starting from Eq. (3); as a result the PCM contribution is split into two terms, namely:

$$\begin{aligned} V_{ai,bj}^{PCM} &= V_{ai,bj}^{ele} + V_{ai,bj}^{dis} \\ &= \int_{\Gamma} ds \sigma[\epsilon_{\infty}, \psi_a^* \psi_i](s) V(\psi_b^* \psi_j)(s) + \beta \int_{\Gamma} ds V(\psi_a^* \psi_i)(s) E(\psi_b^* \psi_j)(s) \end{aligned} \quad (8)$$

In Eq. (8) we have introduced the factor  $\beta$  which, following what reported in Eq. (3), is defined as

$$\beta = k_{dis} \frac{\eta_S^2 - 1}{\eta_S^2} \frac{\Omega^S}{\Omega^S + \omega_{ave}} \quad (9)$$

This factor is however optimized for a ground state system. To extend the same approach to excited states we should recalculate it for each state. Here, however, we have preferred to keep the formulation as the most simple as possible and to introduce a single scaling parameter  $c_s$  for all the excitations which we have determined through a fitting procedure (see below).

We note that the  $\omega_0$  term in Eqs. (4) and (5) can be recovered neglecting  $V_{ai,bj}^{PCM}$  in the resolution of the matrix equation Eq. (6). On the contrary, if we want to determine  $\omega_{SS}$  we have to go a step farther and calculate the relaxation of the ground state electron density due to the excitation. This relaxation contribution can be obtained within the LR-TDDFT scheme in terms of the so-called Z-vector approach<sup>34,35</sup> which has been generalized to the PCM-electrostatic approach by Scalmani et al.<sup>36</sup>. By knowing the resulting electron density, we obtain the second term in the r.h.s. of Eq. (5) by simply calculating the fast component of the PCM surface charge,  $\sigma[\epsilon_\infty, \rho_{\Delta_p}]$ . As a matter of fact, an iterative approach should be introduced in order to obtain mutually equilibrated values of  $\sigma$  and  $\rho_{\Delta_p}$ .<sup>33</sup> However, if we assume that  $\rho_{\Delta_p}$  is small and we note that the correction term in Eq. (5) is quadratic in  $\rho_{\Delta_p}$ , we can just stop at the first-order level of the iteration and obtain what is known as *corrected linear response* (cLR) scheme,<sup>31</sup> which can be seen a first-order approximation to the state-specific excitation energy. **In the present work, the cLR approach is particularly justified, as the electrostatic term in Eq. (5) should be small enough.**

### 3 Computational details

We performed excited state calculations on a set of chromophores presenting different kinds of transitions. Such set includes  $n \rightarrow \pi^*$  chromophores (acetone, acrolein, pyridine, pyrazine, pyrimidine, and pyridazine) and  $\pi \rightarrow \pi^*$  aromatic chromophores (benzene, naphthalene, anthracene).



Geometries were optimized *in vacuo* at the B3LYP/6-311G(d) level of theory, and assumed unchanged upon solvation. For all the calculations, cyclohexane was used as solvent.

The dependence on the density functional was assessed by comparing various functionals, with different weights of exact exchange, and Hartree Fock. All calculations were run using the 6-311+G(2d,2p) split valence basis set.

In order to evaluate the extent of the coupling between the electrostatic and nonelectrostatic interactions, we adopted five different schemes, in which different solute-solvent interactions are included in the PCM effective Hamiltonian. The labels PCM(EDR) refer to the interactions included in the Hamiltonian, where E means *Electrostatic*, D means *Dispersion* and R means *Repulsion*. We employed the M06-2X/6-311+G(2d,2p) level of theory for this and all the following calculations. For the inclusion of electrostatic interactions we employed the two different methods described in the method section, namely LR and cLR

Finally, we parameterized the dispersion contribution to the TDDFT matrices by minimizing the RMS error between the calculated and the experimental solvatochromic shift within the set of selected excitations.

All the calculations were run applying the Tamm-Dancoff approximation (TDA)<sup>37</sup> of the TDDFT formulation and using a locally modified version of the Gaussian09 suite of codes.<sup>38</sup> The electrostatic contribution was obtained using the IEF version<sup>26</sup> of PCM together with a cavity and surface discretization procedure into point charges available in Gaussian09 asking for the Gaussian03 defaults. The molecular cavities were built using Bondi radii scaled by 1.2.

## 4 Results and discussion

### 4.1 Dependence on the DFT functional

As a preliminary analysis we have investigated the dependence of the PCM(EDR) approach on the DFT functional used. In particular, the attention has been focused on the role of the percentage of exact exchange included in the functional. To this aim we have selected 5 functionals, with different weights of exact exchange, LDA,<sup>39,40</sup> PBE<sup>41,42</sup>, B3LYP<sup>43</sup>, M06-2X<sup>44</sup>,  $\omega$ B97X<sup>45</sup>, and HF, together with the 6-311+G(2d,2p) split valence basis set.

As the electrostatic contribution is known to be weakly dependent on the specific functional used, here the analysis has been limited to the dispersion-only description. Moreover, to have a more direct analysis we have focused on “frozen solvent” excitation energies  $\omega_0$ , obtained by including the dispersion contribution only in the ground-state calculation, but not in the response matrices (see Eq. (7)).

**Figure 1** shows the dependence of  $\omega_0$  excitation energies on the percentage of exact exchange in the functional used. We considered the shifts with respect to gas phase, normalized to the shift predicted by the HF method, as in Eq. (10).

$$\Delta\omega_0^{(\text{Norm})} = \frac{\omega_0^{(\text{Func})} - \omega_{\text{vac}}^{(\text{Func})}}{\omega_0^{(\text{HF})} - \omega_{\text{vac}}^{(\text{HF})}} \quad (10)$$

The normalized values were averaged over the first transitions of each chromophore, thus eliminating the dependence on the type of transition.

The variation of  $\omega_0$  excitation energy reflects the variation of the occupied and virtual orbitals in the ground state, and provides information on the Fock dispersion operator.

The behaviour of  $\omega_0$  values is almost linear with the fraction of exact exchange ( $R^2 = 0.9945$ ), and we see a 35% variation of  $\omega_0$  between the two extremes (HF and pure DFs). However, the

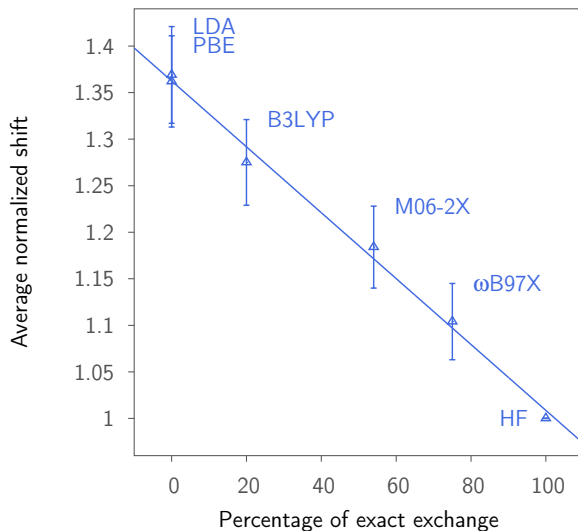


Figure 1: Dependence of the average normalized dispersion shift on the percentage of exact exchange in the functional used. Since  $\omega$ B97X is a *range-separated* hybrid, with the HF exchange ranging from 16% to 100%, we used an “average” value of 75% for the percentage of HF exchange. The error bars represent a standard deviation. The regression line has a slope of  $3.54 \times 10^{-3}$ , an intercept of 1.36 and  $R^2 = 0.9945$

most commonly used functionals fall in the same range, and the difference between B3LYP and M06-2X is only about 8%.

From the results obtained so far, we can guess that the dispersion contribution to the PCM matrix elements,  $V_{ai,bj}^{PCM}$ , and thus its effect on the transition properties, becomes stronger in those functionals that have a small percentage of exact exchange, supposedly because the predicted occupied-virtual orbital energy gap lowers with such functionals, and the dispersion operator implicitly depends on this gap.<sup>28</sup>

For all the following analyses we have selected the M06-2X<sup>44</sup> functional which presents almost 50% of exact exchange: this functional has in fact shown to give very good results for the prediction of electronic excitation energies of main-group compounds by time-dependent density functional theory.<sup>46–48</sup>

## 4.2 Couplings among electrostatic and nonelectrostatic contributions

For each molecule of the set, we report in Figure 2 the dispersion-repulsion coupling ( $\Delta_{DR}$ ), which is defined as the difference between the *gas phase* to cyclohexane solvatochromic shift calculated with the PCM(DR) scheme and the sum of those calculated with the PCM(R) and the PCM(D) schemes. Similarly, the dispersion-repulsion-electrostatic ( $\Delta_{EDR}$ ) coupling is defined as the difference between the PCM(EDR) results and the sum of the PCM(DR) and the PCM(E) contributions.

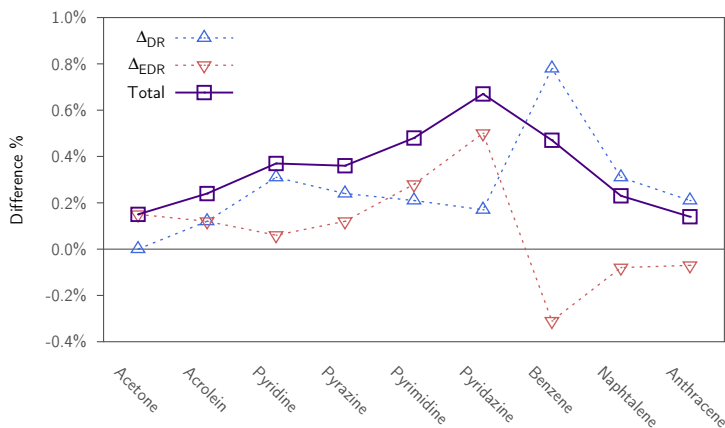


Figure 2: Plot of  $\Delta_{DR}$  and  $\Delta_{EDR}$  as error on the total shift, along with the *total* difference between the PCM(EDR) calculation and the sum of electrostatic, dispersion and repulsion contributions. These values are always less than 1% and therefore negligible.  $\Delta_{DR}$  is defined as  $\frac{\Delta\omega_{DR}-\Delta\omega_D-\Delta\omega_R}{\Delta\omega_{DR}} \times 100\%$ , and  $\Delta_{EDR}$  is defined as  $\frac{\Delta\omega_{EDR}-\Delta\omega_E-\Delta\omega_D-\Delta\omega_R}{\Delta\omega_{EDR}} \times 100\%$

Both  $\Delta_{DR}$  and  $\Delta_{EDR}$  couplings are found to be zero or negligible for any transition we considered. We conclude that the repulsion, dispersion and electrostatic contributions to the excitation energy are almost additive; this allows us to tackle one contribution at a time, and focus the parameterization on the dispersion part only, neglecting its influence on the other contributions. Moreover, we can rely on the quasi additivity of the nonelectrostatic and electrostatic shifts to use the *corrected linear response* scheme for the ES contribution, which will be calculated separately. This result supports the use of models where the solvatochromic shift is calculated as a sum of different (electrostatic and nonelectrostatic) contributions, as in the scheme recently proposed by Marenich *et al.*<sup>21,22</sup> The coupling between electrostatic and nonelectrostatic contribution was found to be

larger but still rather limited (2 to 4%) also for ground-state solvation energies<sup>28</sup>.

### 4.3 The dispersion contribution

As commented in the Methods section, the factor  $\beta$  appearing in the dispersion expression was originally obtained for a ground state solutes ( $k_{dis}$  was optimized with respect to solvation free energies).<sup>20</sup> To adapt the same expression to excitation processes we adopt here a double-step strategy: we use the previously optimized  $\beta$  factor for ground-state calculations and we rescale it with a suitable parameter  $c_s$  when used to calculate the components,  $V_{ai,bj}^{dis}$ , of the PCM response matrix.

Figure 3 shows, as an example, the solvatochromic shift of the  $L_a$  and  $L_b$  transitions of anthracene at different values of the LR operator scaling  $c_s$ .

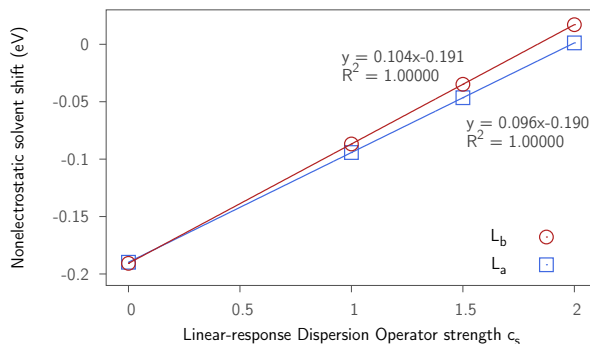


Figure 3: Solvatochromic shift (nonelectrostatic component only) of  $L_a$  and  $L_b$  transitions of Anthracene. The linear fit is also shown for both transitions.

In this case, along with all the other transitions tested, we can see that the behaviour of the excitation energy is perfectly linear in  $c_s$ , so that we can choose a reasonable value for  $c_s$ , which will reduce the errors in the solvatochromic shifts. In order to obtain the optimal  $c_s$  coefficient for each transition, we considered experimental vacuum-to-solvent excitation energy shifts as a reference and found, through the linear calibration curve, the value of  $c_s$  that gives the best agreement.

Although the electrostatic effects are not dominant in nonpolar solvent, we have to include them in

our calculations to make sure that our fitted parameter accounts only for the dispersion contribution to the excitation energy shift. As reported in the Methods Section, there are alternative approaches for the inclusion of electrostatic effects in an excitation process. Here, we focus on the LR and cLR models. **Finally, the contribution from repulsion was included in all the calculations.**

We took as references the experimental *gas phase* to cyclohexane spectral shifts, where they were available, or to another similar solvent. The chromophores used in the parameterization are listed in Table 1 along with the experimental shifts; **the calculated *gas-phase* transition energies and experimental absorption maxima are given in table S5.** It should be noted that this comparative procedure presents an intrinsic uncertainty, because the calculated quantity, a shift in the *vertical excitation energy*, is not directly available experimentally. The shift in the band maximum is commonly used to approximate the variation in vertical excitation energies, but the uncertainty in the comparison should be kept in mind, especially since we want to use this comparison to fit an empirical parameter to use in our model. For this reason, we also estimated an error in the value of  $c_s$  assuming that there is an uncertainty of  $50 \text{ cm}^{-1}$  in the experimentally derived shifts.

**Table 1: The chromophores and transitions employed for the parameterization, along with the experimental vacuum to solvent shifts ( $\text{cm}^{-1}$ ). When the shifts were not available, we took the solvent shift as the difference in the most intense vibronic peak in gas-phase and solvent spectra. If not reported differently, gas-phase data are from Ref.<sup>58</sup>.**

Chromophore	Transition	$\Delta\omega$ (exptl.)	Notes
Acetone	$n\pi^*$	-55	<i>In n-decane</i> <sup>49</sup>
Pyridine	$\pi\pi^*$	-325	<i>In isooctane</i> <sup>50</sup> .
Pyrazine	$n\pi^*$	-400	<i>In cyclohexane</i> <sup>51</sup> .
	$\pi\pi^*$	-550	
Pyrimidine	$n\pi^*$	-200	<i>In cyclohexane</i> <sup>52</sup> .
	$\pi\pi^*$	-320	<i>In methylcyclohexane</i> <sup>53</sup> .
Pyridazine	$\pi\pi^*$	-130	<i>In cyclohexane</i> <sup>51</sup> <b>and vacuo</b> <sup>54</sup> .
Benzene	$L_b$	-308	<i>From Ref.</i> <sup>55</sup>
	$L_a$	-1070	
Naphtalene	$L_b$	-296	<i>From Ref.</i> <sup>56</sup>
	$L_a$	-954	
Anthracene	$L_a$	-1030	<i>From Ref.</i> <sup>57</sup>
	$B_b$	-2917	

We choose the parameter  $c_s$  by minimizing the RMS error  $E$  between the calculated and the experimental shift within the set presented in Table Table 1:

$$E = \sqrt{\frac{\sum_k (\Delta\omega_k^{\text{calc.}} - \Delta\omega_k^{\text{exp.}})^2}{N}}$$

$\Delta\omega_k^{\text{calc.}}$  is a function of the only parameter  $c_s$ . Since the behaviour of  $\Delta\omega$  for all the transitions is perfectly linear with  $c_s$ , we can write  $\Delta\omega_k^{\text{calc.}} = a_k + b_k \cdot c_s$ , and find analytically the optimal value for  $c_s$ .

We report in Table Table 2 the optimal  $c_s$  values, calculated using two different schemes for electrostatic, LR and cLR, along with the RMS and maximum absolute error.

**Table 2: Results for the fitting of the  $c_s$  parameter, employing two different schemes for the electrostatic contribution. RMS and MAE values are in  $\text{cm}^{-1}$ .**

Model	Optimal $c_s$	RMS error	MAE
LR	1.510±0.005	295	759
cLR	1.232±0.005	368	837

We see that the both schemes yield  $c_s > 1$  even if with fairly different values and with the LR scheme giving slightly smaller errors. A fitted  $c_s > 1$  is not unexpected. In fact, for a solvated molecule in an excited state, the dispersion energy receives a contribution also from de-excitations. By adopting a simplified scheme, we can write from Eq. (3)

$$\frac{c_s}{\Omega^S + \omega_{ave}} \approx \frac{p_I}{\Omega^S + \omega_{ave}^I} + \frac{p_{II}}{\Omega^S + \omega_{ave}^{II}} \quad (11)$$

in which we distinguish explicitly two contributions to the average, one from excitations to higher energy states ( $I$ ) and one from de-excitations to lower energy states ( $II$ ). By putting  $\omega_{ave}^I + \omega_{ave}^{II} = \omega_{ave}$  and assuming for the weight a simple expression like  $p_I = \omega_{ave}^I / \omega_{ave}$ , we have almost immediately

$$c_s \approx \frac{p_I(\Omega^S + \omega_{ave})}{\Omega^S + p_I\omega_{ave}} + \frac{(1 - p_I)(\Omega^S + \omega_{ave})}{\Omega^S - (1 - p_I)\omega_{ave}} \quad (12)$$

This equation leads to  $c_s = 1$  when  $p_I = 1$  and  $c_s > 1$  when  $p_I < 1$  in agreement with our finding. This simple analysis also tells us also that  $c_s$  should depend on the solvent through  $\Omega^S$ .

To assess if our model is capable of reproducing the trend in solvent shifts, we report, for both LR and cLR schemes, the correlation plots between experimental and calculated shifts (Figure 4).

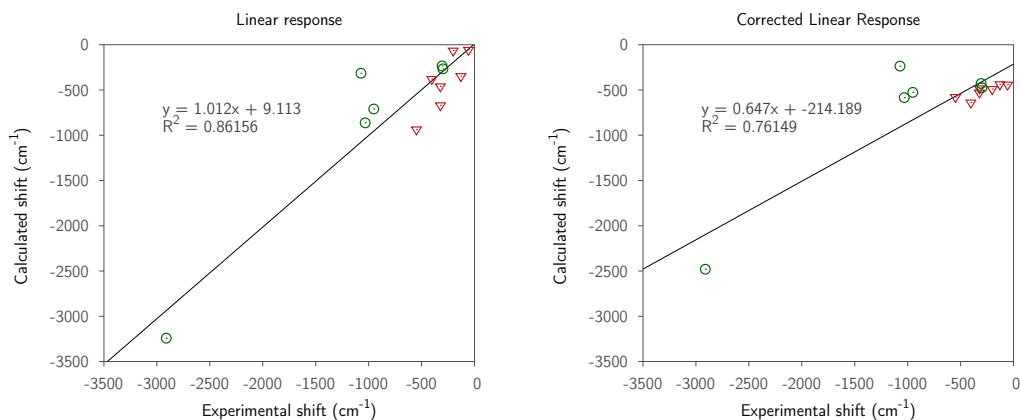


Figure 4: Correlation of experimental and calculated solvent spectral shifts ( $\text{cm}^{-1}$ ). The plot on the left was obtained using the *Linear response* (LR) scheme for the electrostatic contribution, and the plot on the right was obtained using the *Corrected Linear response* (cLR) scheme. Circles represent nonpolar aromatic hydrocarbons (benzene, naphthalene, anthracene), while triangles represent polar chromophores (acetone, pyridine and diazines)

From the analysis of these plots we can make some considerations. Firstly, the LR electrostatic scheme better differentiates between the various transitions, while the cLR scheme yields shifts that are too similar, resulting in a smaller correlation between calculated and experimental values. Secondly, we can recognize two sets of transitions, denoted with different marks in the plot; one includes nonpolar chromophores (benzene, naphthalene and anthracene, only  $\pi \rightarrow \pi^*$  transitions), whose shifts are typically underestimated by our model, while the other includes polar chromophores (acetone, pyridine and the diazines, with both  $\pi \rightarrow \pi^*$  and  $n \rightarrow \pi^*$  transitions), whose shifts are overestimated. We also note that there is one particular transition, the  $L_a$  transition of benzene, that appears to be an outlier, as it lies too far from the nonpolar trendline and corresponds to the maximum error between calculated and experimental shift in both electrostatic schemes: this transition is the responsible of the MAE values of  $759 \text{ cm}^{-1}$  (LR) and  $857 \text{ cm}^{-1}$  (cLR) reported in Table 2. The unexpectedly low red shift predicted by our model for benzene  $L_a$



can be partially explained in terms of an overestimation of the repulsion component, which corresponds to a blue shift of  $320 \text{ cm}^{-1}$  (See Supporting Info). This may be due to a mixing of  $\pi \rightarrow \pi^*$  and Rydberg states in the TD-DFT description of this transition.

## 4.4 Discussion

To investigate deeper the results obtained above, we summarize here the analysis done by Corni *et al.*<sup>59</sup> based on a simple model for the solute-solvent system that bypasses one of the basic assumptions of continuum solvation models, i.e., the use of a single Hartree product of a solute and a solvent wave function to describe the total solute-solvent wave function. In such an analysis the total wave function was described as a linear combination of the four products of two solute states and two solvent electronic states. The solute excitation energy resulting from such an analysis is here rewritten in a form which is reminiscent of the Onsager model for solute-solvent interactions (a dipolar solute in a spherical cavity):

$$\begin{aligned} \omega &= \omega_0 - \frac{1}{2}g_e(\mu_{GS} - \mu_{ES})^2 - g_e^d |\mu^T|^2 - \frac{1}{2\pi} \int_0^\infty d\omega g(i\omega)\Delta\alpha(i\omega) \\ &= \omega_0 - \omega_{\text{Ele}} - \omega_{\text{Res}} - \omega_D \end{aligned} \tag{13}$$

where  $g_e$  is the linear electronic response of the solvent (and it can be interpreted as the Onsager-like nonequilibrium response function of the solvent),  $\mu_{GS}$  and  $\mu_{ES}$  are the ground and excited-state electric dipoles of the solute, and  $\mu^T$  is the transition dipole between them.

As already commented, the first term on r.h.s. of Eq. (13),  $\omega_0$ , takes into account the polarization of the solvent with respect to the ground-state electron density; the second term contains the square of the difference between the response of the solvent electronic polarization to the ground and excited state densities, and is a purely electrostatic term. The third term depends on the transition density between ground and excited state (that is, in a dipolar approximation, to the square of the transition dipole); this contribution, which we shall call “resonance” term, is identifiable with

the Bayliss equation for the spectral shift in nonpolar solvents,<sup>17</sup> and is sometimes considered a dispersion effect<sup>18,59,60</sup> The last term is the “pure” dispersion term, namely the difference in dispersion energies of ground and excited states. We also note that the last three terms depend on the same solvent parameter  $\epsilon_\infty$ . In polar solvents,  $\omega_0$  is the dominant one, because it is the only term that is determined by the full response of the solvent (including also the orientational polarization). However, in nonpolar solvents, all four terms can be of the same magnitude.

By comparing Eq. (13) with the LR and cLR ones (Eqs. (4) and (5)), it is evident that the LR and the cLR schemes contain different subsets of the total number of terms. In particular, the cLR model, as expected from its purely electrostatic nature, includes only the first and the second term (or better a first-order approximation of that), while the LR, unexpectedly, includes the first and the third term even if the latter is not a real electrostatic term. In the original analysis, the LR “ambiguity” was related to the incapability of the effective Hamiltonian of QM continuum models to correctly describe energy expectation values of not stationary solute states. Since in a perturbation approach, such as the LR treatment, the perturbed state can be seen as a linear combination of zeroth-order states, a wrong partition of the solvent terms among the various perturbation orders is obtained. In the same analysis, the LR contribution was described as part of the dispersion term together with the “pure” one.

The present analysis seems to confirm this physical interpretation for the following reasons. When a nonpolar solvent is considered, the electrostatic contribution is expected to be rather small if not negligible (especially if the transition does not lead to significant electron density variations). As a result the cLR contribution when combined to the “pure” dispersion term should not change the correlations between calculated and experimental gas-to-nonpolar shifts. On the contrary, the combination of “resonance” and “pure” dispersion contribution (i.e. the coupling of dispersion and LR results) should give a better estimation of the real solvent effects as they both account for nonelectrostatic effects. This is indeed what we have observed in the graphs reported in Figure 4.

**We note that models which introduce semiempirical corrections of the excitation energies naturally**

include the “resonance” and “pure” dispersion contributions.<sup>21,61,62</sup>

## 5 Summary

In this paper we have investigated the limits and potentialities of PCM in describing gas-to-nonpolar solvent shift of excitation energies for solvated systems. The analysis has been performed combining electrostatic and nonelectrostatic terms in the solute effective Hamiltonian and in the resulting TD-DFT equations (here applied in their TDA version). The results obtained using a reparameterized version of the Amovilli and Mennucci dispersion formulation<sup>12</sup> seem to show that in nonpolar solvents the role of electrostatic effects is almost null, as expected, but that instead the inclusion of the so-called “resonance” contribution can significantly improve the correlation with experiments. This term in the literature has been already included in the dispersion contribution<sup>17,18,59,60</sup> but in most of the continuum model calculations represents the electrostatic response to the solute electronic transition. Our analysis seems to confirm the first interpretation and it suggests that the so-called LR formulation of continuum models for electronic excitations should be taken with care as it introduces a nonelectrostatic response which, if treated alone, could lead to unbalanced effects. On the contrary, the cLR, or other SS approaches, are much safer approaches to include electrostatic responses and they can be always combined with dispersion (and repulsion) models possibly including also the “resonance” term.<sup>22</sup>

## Acknowledgement

L.C. and B.M. acknowledge the European Research Council (ERC) for financial support in the framework of the Starting Grant (EnLight - 277755).

## Supporting Information

Dispersion-induced excitation energy shifts used to obtain Figure 1; Excitation energy shifts calcu-

lated with different PCM schemes used to obtain Figure 3; DR component of the excitation energy shifts (eV), at different values of the fitting parameter  $c_s$ ; Electrostatic and nonelectrostatic components of the excitation energy shifts. This material is available free of charge via the Internet at <http://pubs.acs.org>.

## References

- (1) Warshel, A.; Levitt, M. Theoretical studies of enzymic reactions: dielectric, electrostatic and steric stabilization of the carbonium ion in the reaction of lysozyme. *J. Mol. Biol.* **1976**, *103*, 227–249.
- (2) Field, M. J.; Bash, P. A.; Karplus, M. A combined quantum mechanical and molecular mechanical potential for molecular dynamics simulations. *J. Comput. Chem.* **1990**, *11*, 700–733.
- (3) Gao, J. Hybrid quantum and molecular mechanical simulations: An alternative avenue to solvent effects in organic chemistry. *Accounts Chem. Res.* **1996**, *29*, 298–305.
- (4) Lin, H.; Truhlar, D. G. QM/MM: what have we learned, where are we, and where do we go from here? *Theor. Chem. Acc.* **2007**, *117*, 185–199.
- (5) Senn, H. M.; Thiel, W. QM/MM methods for biomolecular systems. *Angew. Chem. Int. Edit.* **2009**, *48*, 1198–1229.
- (6) Olsen, J. M. H.; Kongsted, J. In *Chapter 3 - Molecular Properties through Polarizable Embedding*; Sabin, J. R., Brändas, E., Eds.; Advances in Quantum Chemistry; Academic Press, 2011; Vol. 61; pp 107 – 143.
- (7) Rivail, J. L.; Rinaldi, D. A quantum chemical approach to dielectric solvent effects in molecular liquids. *Chem. Phys.* **1976**, *18*, 233–242.
- (8) Tomasi, J.; Persico, M. Molecular-Interactions In Solution - An Overview Of Methods Based On Continuous Distributions Of The Solvent. *Chem Rev* **1994**, *94*, 2027–2094.

- (9) Cramer, C.; Truhlar, D. Implicit solvation models: Equilibria, structure, spectra, and dynamics. *Chem. Rev.* **1999**, *99*, 2161–2200.
- (10) Orozco, M.; Luque, F. J. Theoretical Methods for the Description of the Solvent Effect in Biomolecular Systems. *Chem. Rev.* **2000**, *100*, 4187–4226.
- (11) Tomasi, J.; Mennucci, B.; Cammi, R. Quantum mechanical continuum solvation models. *Chem. Rev.* **2005**, *105*, 2999–3093.
- (12) Amovilli, C.; Mennucci, B. Self-Consistent-Field Calculation of Pauli Repulsion and Dispersion Contributions to the Solvation Free Energy in the Polarizable Continuum Model. *J. Phys. Chem. B* **1997**, *101*, 1051–1057.
- (13) Pomogaeva, A.; Chipman, D. M. New implicit solvation models for dispersion and exchange energies. *J. Phys. Chem. A* **2013**, *117*, 5812–20.
- (14) Pomogaeva, A.; Chipman, D. M. Hydration Energy from a Composite Method for Implicit Representation of Solvent. *Journal of Chemical Theory and Computation* **2014**, *10*, 211–219.
- (15) Mennucci, B. Polarizable continuum model. *Wiley Interdiscip. Rev. Comput. Mol. Sci.* **2012**, *2*, 386–404.
- (16) Barone, V.; Baiardi, A.; Biczysko, M.; Bloino, J.; Cappelli, C.; Lipparini, F. Implementation and validation of a multi-purpose virtual spectrometer for large systems in complex environments. *Phys. Chem. Chem. Phys.* **2012**, *14*, 12404–12422.
- (17) Bayliss, N. The effect of the electrostatic polarization of the solvent on electronic absorption spectra in solution. *J. Chem. Phys.* **1950**, *18*, 292–296.
- (18) Roesch, N.; Zerner, M. Calculation of dispersion energy shifts in molecular electronic spectra. *J. Phys. Chem.* **1994**, 5817–5823.

- (19) Renger, T.; Grundkötter, B.; Madjet, M. E.-A.; Müh, F. Theory of solvatochromic shifts in nonpolar solvents reveals a new spectroscopic rule. *Proc. Natl. Acad. Sci. U. S. A.* **2008**, *105*, 13235–13240.
- (20) Weijo, V.; Mennucci, B.; Frediani, L. Toward a General Formulation of Dispersion Effects for Solvation Continuum Models. *J. Chem. Theory Comput.* **2010**, *6*, 3358–3364.
- (21) Marenich, A. V.; Cramer, C. J.; Truhlar, D. G. Uniform Treatment of Solute–Solvent Dispersion in the Ground and Excited Electronic States of the Solute Based on a Solvation Model with State-Specific Polarizability. *J. Chem. Theory Comput.* **2013**, 3649–3659.
- (22) Marenich, A. V.; Cramer, C. J.; Truhlar, D. G. Electronic Absorption Spectra and Solvatochromic Shifts by the Vertical Excitation Model: Solvated Clusters and Molecular Dynamics Sampling. *J. Phys. Chem. B* **2014**, doi:10.1021/jp506293w.
- (23) Miertus, S.; Scrocco, E.; Tomasi, J. Electrostatic interaction of a solute with a continuum. A direct utilization of ab-initio molecular potentials for the prevision of solvent effects. *Chem. Phys.* **1981**, *55*, 117 – 129.
- (24) Cammi, R.; Tomasi, J. Remarks on the use of the apparent surface charges (ASC) methods in solvation problems: Iterative versus matrix-inversion procedures and the renormalization of the apparent charges. *J. Comput. Chem.* **1995**, *16*, 1449–1458.
- (25) Barone, V.; Cossi, M. Quantum calculation of molecular energies and energy gradients in solution by a conductor solvent model. *J Phys Chem A* **1998**, *102*, 1995–2001.
- (26) Cancès, E.; Mennucci, B.; Tomasi, J. A New Integral Equation Formalism for the Polarizable Continuum Model: Theoretical Background and Applications to Isotropic and Anisotropic Dielectrics. *J. Chem. Phys.* **1997**, *107*, 3032–3041.
- (27) Amovilli, C. Calculation of the dispersion energy contribution to the solvation free energy. *Chem. Phys. Lett.* **1994**, *229*, 244–249.

- (28) Curutchet, C.; Orozco, M.; Luque, F. J.; Mennucci, B.; Tomasi, J. Dispersion and repulsion contributions to the solvation free energy: comparison of quantum mechanical and classical approaches in the polarizable continuum model. *J. Comput. Chem.* **2006**, *27*, 1769–1780.
- (29) Cammi, R.; Mennucci, B. Linear response theory for the polarizable continuum model. *J. Chem. Phys.* **1999**, *110*, 9877–9886.
- (30) Cossi, M.; Barone, V. Time-dependent density functional theory for molecules in liquid solutions. *J. Chem. Phys.* **2001**, *115*, 4708–4717.
- (31) Caricato, M.; Mennucci, B.; Tomasi, J.; Ingrosso, F.; Cammi, R.; Corni, S.; Scalmani, G. Formation and relaxation of excited states in solution: A new time dependent polarizable continuum model based on time dependent density functional theory. *J Chem Phys* **2006**, *124*, 124520–124513.
- (32) Impropa, R.; Barone, V.; Scalmani, G.; Frisch, M. J. A state-specific polarizable continuum model time dependent density functional theory method for excited state calculations in solution. *J Chem Phys* **2006**, *125*, 054103.
- (33) Marenich, A. V.; Cramer, C. J.; Truhlar, D. G.; Guido, C. A.; Mennucci, B.; Scalmani, G.; Frisch, M. J. Practical computation of electronic excitation in solution: vertical excitation model. *Chem. Sci.* **2011**, *2*, 2143–2161.
- (34) Handy, N. C.; Schaefer, H. F. On the evaluation of analytical energy derivatives for correlated wave functions. *J Chem Phys* **1984**, *81*, 5031–5033.
- (35) Foresman, J.; Head-Gordon, M.; Pople, J.; Frisch, M. Toward A Systematic Molecular-Orbital Theory For Excited-States. *J Phys Chem-US* **1992**, *96*, 135–149.
- (36) Scalmani, G.; Frisch, M.; Mennucci, B.; Tomasi, J.; Cammi, R.; Barone, V. Geometries and properties of excited states in the gas phase and in solution: Theory and application of a time-

- dependent density functional theory polarizable continuum model. *J. Chem. Phys.* **2006**, *124*, 094107–094115.
- (37) Hirata, S.; Head-Gordon, M. Time-dependent density functional theory within the Tamm–Dancoff approximation. *Chem Phys Lett* **1999**, *314*, 291–299.
- (38) Frisch, M. J. et al. Gaussian 09 Revision D.01. Gaussian Inc. Wallingford CT 2009.
- (39) Slater, J. Comparison of TFD and  $X\alpha$  methods for molecules and solids. *Int. J. Quantum Chem. Symp.* **195**, *9*, 7–21.
- (40) Vosko, S. H.; Wilk, L.; Nusair, M. Accurate spin-dependent electron liquid correlation energies for local spin density calculations: A critical analysis. *Can. J. Phys.* **1980**, *58*, 1200–1211.
- (41) Perdew, J. P.; Burke, K.; Ernzerhof, M. Generalized Gradient Approximation Made Simple. *Phys. Rev. Lett.* **1996**, *77*, 3865–3868.
- (42) Perdew, J. P.; Burke, K.; Ernzerhof, M. Generalized Gradient Approximation Made Simple [Phys. Rev. Lett. *77*, 3865 (1996)]. *Phys. Rev. Lett.* **1997**, *78*, 1396–1396.
- (43) Becke, A. D. Density-functional thermochemistry. III. The role of exact exchange. *J. Chem. Phys.* **1993**, *98*, 5648–5652.
- (44) Zhao, Y.; Truhlar, D. G. The M06 suite of density functionals for main group thermochemistry, thermochemical kinetics, noncovalent interactions, excited states, and transition elements: two new functionals and systematic testing of four M06-class functionals and 12 other functionals. *Theor. Chem. Acc.* **2008**, *120*, 215–241.
- (45) Chai, J.-D.; Head-Gordon, M. Systematic optimization of long-range corrected hybrid density functionals. *J. Chem. Phys.* **2008**, *128*, 084106.



- (46) Jacquemin, D.; Perpète, E. A.; Ciofini, I.; Adamo, C.; Valero, R.; Zhao, Y.; Truhlar, D. G. On the Performances of the M06 Family of Density Functionals for Electronic Excitation Energies. *J Chem Theory Comput* **2010**, *6*, 2071–2085.
- (47) Li, R.; Zheng, J.; Truhlar, D. G. Density functional approximations for charge transfer excitations with intermediate spatial overlap. *Phys Chem Chem Phys* **2010**, *12*, 12697.
- (48) Leang, S. S.; Zahariev, F.; Gordon, M. S. Benchmarking the performance of time-dependent density functional methods. *J Chem Phys* **2012**, *136*, 104101.
- (49) Renge, I. Solvent dependence of  $n\text{-}\pi^*$  absorption in acetone. *J. Phys. Chem. A* **2009**, *113*, 10678–10686.
- (50) Stephenson, H. P. Solution Spectra and Oscillator Strengths of Electronic Transitions of Pyridine and Some Monosubstituted Derivatives. *J. Chem. Phys.* **1954**, *22*, 1077–1082.
- (51) Halverson, F.; Hirt, R. C. Near Ultraviolet Solution Spectra of the Diazines. *J. Chem. Phys.* **1951**, *19*, 711–718.
- (52) Baba, H.; Goodman, L.; Valenti, P. C. Solvent Effects on the Fluorescence Spectra of Diazines. Dipole Moments in the ( $n,\pi^*$ ) Excited States 1. *J. Am. Chem. Soc.* **1966**, *88*, 5410–5415.
- (53) Clark, L. B.; Tinoco, I. Correlations in the Ultraviolet Spectra of the Purine and Pyrimidine Bases. *J. Am. Chem. Soc.* **1965**, *87*, 11–15.
- (54) Holland, D. M. P.; Shaw, D. a.; Coriani, S.; Stener, M.; Decleva, P. A study of the valence shell electronic states of pyridazine by photoabsorption spectroscopy and time-dependent density functional theory calculations. *Journal of Physics B: Atomic, Molecular and Optical Physics* **2013**, *46*, 175103.
- (55) Bayliss, N.; Hulme, L. Solvent effects in the spectra of Benzene, Toluene, and Chlorobenzene at 2600 and 2000 Å. *Aust. J. Chem.* **1953**, *6*, 257–277.

- (56) Weigang, O. E. Spectral Solvent Shift. I. Paraffin Hydrocarbon Solvent Interactions with Polynuclear Aromatic Hydrocarbons. *J. Chem. Phys.* **1960**, *33*, 892–899.
- (57) Morales, R. G. E. Polarizability change in the excited electronic states of nonpolar aromatic hydrocarbons. *J. Phys. Chem.* **1982**, *86*, 2550–2552.
- (58) Bolovinos, A.; Tsekeris, P.; Philis, J.; Pantos, E.; Andritsopoulos, G. Absolute vacuum ultraviolet absorption spectra of some gaseous azabenzenes. *J. Mol. Spectrosc.* **1984**, *103*, 240–256.
- (59) Corni, S.; Cammi, R.; Mennucci, B.; Tomasi, J. Electronic excitation energies of molecules in solution within continuum solvation models: investigating the discrepancy between state-specific and linear-response methods. *J. Chem. Phys.* **2005**, *123*, 134512.
- (60) Zhu, C.; Dalgarno, A.; Porsev, S.; Derevianko, A. Dipole polarizabilities of excited alkali-metal atoms and long-range interactions of ground- and excited-state alkali-metal atoms with helium atoms. *Phys. Rev. A* **2004**, *70*, 032722.
- (61) Li, J.; Cramer, C. J.; Truhlar, D. G. Two-response-time model based on CM2/INDO/S2 electrostatic potentials for the dielectric polarization component of solvatochromic shifts on vertical excitation energies. *Int. J. Quantum Chem.* **2000**, *77*, 264–280.
- (62) Marenich, A. V.; Cramer, C. J.; Truhlar, D. G. Sorting Out the Relative Contributions of Electrostatic Polarization, Dispersion, and Hydrogen Bonding to Solvatochromic Shifts on Vertical Electronic Excitation Energies. *J. Chem. Theory and Comput.* **2010**, *6*, 2829–2844.

## Graphical TOC Entry

